Since January 2020 Elsevier has created a COVID-19 resource centre with free information in English and Mandarin on the novel coronavirus COVID-19. The COVID-19 resource centre is hosted on Elsevier Connect, the company's public news and information website.

International Journal of Biological Macromolecules 94 (2017) 290–300

Contents lists available at ScienceDirect

International Journal of Biological Macromolecules

journal homepage: www.elsevier.com/locate/ijbiomac

Research article

Polyols (Glycerol and Ethylene glycol) mediated amorphous aggregate inhibition and secondary structure restoration of metalloproteinase-conalbumin (ovotransferrin)

Mohsin Vahid Khan[a], Mohd Ishtikhar[a], Gulam Rabbani[a], Masihuz Zaman[a], Ali Saber Abdelhameed[b], Rizwan Hasan Khan[a,*]

[a] Molecular Biophysics and Biophysical Chemistry Group, Interdisciplinary Biotechnology Unit, Aligarh Muslim University, Aligarh, 202002, India
[b] Department of Pharmaceutical Chemistry, College of Pharmacy, King Saud University, Riyadh, 11451, Saudi Arabia

ARTICLE INFO

Article history:
Received 7 October 2016
Accepted 10 October 2016
Available online 12 October 2016

Keywords:
Amorphous aggregates
Conalbumin
Congo red
Dynamic light scattering
Electron microscopy

ABSTRACT

Under physical or chemical stress, proteins tend to form aggregates either highly ordered (amyloid) or unordered (amorphous) causing many pathological disorders in human and loss of proteins functionality in both laboratory conditions and industries during production and storage at commercial level. We investigated the effect of increasing temperature on Conalbumin (CA) and induced aggregation at 65 °C. The enhanced Thioflavin T (ThT) and ANS (1-anilinonaphtalene 8-sulfonic acid) fluorescence intensity, show no shift on Congo red binding, additionally, transmission and scanning electron microscopy (TEM) (SEM) reveal amorphous morphology of the aggregate. Our investigation clearly demonstrated that polyols namely Glycerol (GL) and Ethylene glycol (EG) are so staunch to inhibit amorphous aggregates *via* restoring secondary conformation. Addition of polyols (15% GL and 35% EG) significantly decrease the turbidity, Rayleigh scattering ThT and ANS fluorescence intensity. The dynamic light scattering (DLS) data show that hydrodynamic radii (R_h) of the aggregates is ~20 times higher than native CA while nearly similar for GL and EG protected CA due to condensation of core size with little difference.

1. Introduction

The intricate mode and processes involved in the induction and inhibition of protein aggregation bear great interest in the field of biotechnology, therapeutics, food and pharmaceutical industries. In destabilizing conditions, proteins tend to form aggregates either amorphous or amyloids as a consequence of the achieved intermediate states by unfolding or misfolding. Such conformational aberrations are highly linked with many pathological disorders [1,2]. The hydrophobic and hydrophilic forces established between solvent and protein molecules possess a principle impact on the conformation stabilization of proteins.

The product of proteins unfolding or misfolding lead to the exposure of hydrophobic patches which offers to interact through and leads to the formation of firm complex *via* transformation of soluble monomeric entities to large insoluble ones [3]. The establishment of novel interactions in the protein molecule occurs due to enhanced exposure of thiol groups or hydrophobic patches to thermally induced aggregation [4]. The cataract disease for instance is a result of aggregation of a γD-crystalline protein which has been categorized as amorphous in nature [5], similarly Fanconi syndrome [6], light-chain deposition disease (LCDD), and myeloma nephropathy [7]. While, Alzheimer's, Parkinson's, spongiform encephalopathies, and type II diabetes mellitus [1,2,8] are amyloid aggregates. In the production of bacterial recombinant proteins, the formed inclusion bodies are also classified as amorphous aggregates. It is an outcome of the accumulation of excessively produced polypeptides followed by the unavailability of sufficient chaperons to govern the folding process to rescue from aggregation and restoration of nascent peptides [9,10]. In a similar vein in liquor industry, the amorphous aggregate formation takes place in the form of protein haze during the course of white wine production [11]. Thermally induced aggregation is one of the most studied factors where several proteins have been reported to have undergone the process of aggregate formation at elevated temperature but the effective temperature and duration of incubation fluctuates from protein to protein. For instance, a slight increase in the temperature (~37 °C) can cause aggregation of the Apo form of muscle glycogen phosphorylase b

* Corresponding author at: Interdisciplinary Biotechnology Unit Aligarh Muslim University, Aligarh 202 002, India.
E-mail addresses: rizwanhkhan@hotmail.com, rizwanhkhan1@yahoo.com, rizwanhkhan1@Gmail.com (R.H. Khan).

http://dx.doi.org/10.1016/j.ijbiomac.2016.10.023
0141-8130/

(apoPhb) of rabbit origin [12], while Aquaporin 0 (AQP0) aggregates at 60 °C [13], bovine hemoglobin aggregates at ~70 °C [14], recombinant human interferon alpha2b (rhIFNα2b) aggregates at 50 °C [15] while SARS-associated corona virus (SARS-CoV) protein aggregates at most extreme condition *i.e.* boiling temperature [16]. Thermal and cetyltrimethylammonium bromide [14], NaCl [17], acidic pH [18], metal [19], atheronal-A, atheronal-B, cholesterol [20], Rosin modified surfactant, (QMRAE) [21], non-fluorinated and fluorinated cosolvents [22] are few examples of physical as well as chemical inducer where protein unambiguously forms amorphous aggregate. While, cationic surfactant like CTAB induce amyloid fibrils in stem bromelain [23].

Oligomers of Aβ responsible for the synaptic dysfunction, upon their interaction with fragment of prion protein N-terminal (PrPN1), they modify the conformation which finally result in amorphous aggregate formation [24].

From a therapeutic perspective, it is quite obligatory to design and generate idea which can combat the aggregation inducing factors and protect the proteins *in vivo* as well as *in vitro*. In such trend, that dual function has been displayed by quercetin for the conformation conservation of insulin, which inhibits the fibril formation and also shows disorganizing ability by amyloid fibril (ordered structure) conversion into amorphous aggregates (unordered structure) [25]. In this series, clofazimine inhibits as well as destabilize the fibrils of hen egg white lysozyme [26]. Moreover, Aspartate-β-semi aldehyde dehydrogenase forms aggregates, *via* soluble to insoluble polymerization as function of concentration and time. Lumry–Eyring with nucleated polymerization (LENP) model revealed that increasing concentrations of glycerol inhibits the formation of insoluble, high molecular weight aggregates by delaying the polymerization [27]. The weak polarity-reducing property of ethylene glycol curtails the interaction between hydrocarbon spacer arm mediated nonspecific interaction of N^6-(6-Aminohexyl)-AMP and functional hydrophobic sites present on the pig heart lactate dehydrogenase. The low concentration of ethylene glycol achieves high retrieval of enzymatic activity along with increased yield of enzyme during chromatographic elution within the concentration range of 20–30% (v/v) [28]. Fat as additive used for prion, fetches the more trifling condition for its inactivation, while, glycerol provides stability to the prion 27–30 or prion rods during heat treatment by shielding the peptide backbone [29]. An earlier study on reversing the impact on mutant archetype of Familial Creutzfeldt–Jakob disease (CJD) H187R, has confirmed that glycerol effectively diminishes the PrP187R accumulation in lysosomes of transfected cells followed by transportation up to the cell surface [30].

Furthermore, the osmolytes are known to affect the kinetics and lengthen the lag phase of amyloid but this effect does not solely depend on the viscosity of cosolutes. Despite of viscosity difference between sorbitol and glycerol, both can enhance the lag phase by more than two folds but triethylene glycol (viscosity similar to glycerol) and polyethylene glycol (PEG-400) (with highest viscosity), shorten the lag phase [31].

Conalbumin (ovotransferrin, metalloproteinase) is a glycoprotein made up single polypeptide chain; it is comprised of 686 amino acid residues, holding high affinity sites for iron binding. The two iron binding sites are distributed in comparable tertiary structure of each lobes "N" (1–332) and "C" (342–686) [32]. Ovotransferrin exhibits killer activities against a wide range of microorganisms [33,34]. Further, immunomodulation [35], anti-oxidative [36] and anti-carcinogenicity [37] are the other significant biological activities associated with ovotransferrin. The primary goal of the current study is to induce aggregation in CA by thermal treatment and characterization the type of aggregates. Further, we checked the protective and anti-aggregation property of glycerol (GL) and ethylene glycol (EG) at 65 °C. To the best of our knowledge, no previous studies reported the GL and EG mediated inhibition of thermally induced amorphous aggregates by a multi-technique approach.

2. Materials and methods

2.1. Materials

Iron-free conalbumin from chicken egg white (C 0755), Thioflavin T (T 3516), ANS (A 10288) and Congo red (CR) were purchased from Sigma Chemical Co. (St. Louis, Mo, USA). Extrapure glycerol (072929) and ethylene glycol (05291) was purchased from SISCO research laboratories Pvt. Limited, Mumbai, India. All other reagents and buffer compounds used were of analytical grade.

2.2. Concentration determination of protein

Protein stock was prepared in 20 mM sodium phosphate buffer pH 7.0, and concentration was measured by using the extinction coefficient at $E^{1\%}_{280nm} = 12.0$ on Perkin Elmer (Lambda 25) double beam spectrophotometer attached with peltier temperature programmer (PTP-1). A filtered buffer through a 0.45 μm Millipore Millex-HV PVDF filter was used throughout the study.

2.3. Turbidity measurements

Turbidity measurements were performed on a Perkin Elmer UV–vis spectrometer model lambda 25 in a cuvette of 1 cm path length. All the measurements of protein sample with increasing concentration (v/v) of polyols were monitored by measuring absorbance at 350 nm at room temperature. Conalbumin (5 μM) was incubated for 60 min in both the conditions, for thermal range 25–85 °C and on increasing concentrations of GL and EG at 65 °C.

2.4. Rayleigh light scattering (RLS) measurements

Rayleigh scattering measurements were carried on a Shimadzu spectrophotometer RF-5301 PC at 25 ± 0.1 °C with a 1 cm path length cell. The protein samples incubated with increasing concentrations of polyols (GL and EG) were excited at 350 nm and spectra were recorded over the wavelength range of 300–400 nm. The data were plotted at 350/350 nm. Conalbumin (5 μM) was incubated for 60 min in both the conditions, for thermal range 25–85 °C and on increasing concentration of GL and EG at 65 °C.

2.5. Tryptophan fluorescence measurements

Fluorescence measurements were performed on a Shimadzu spectrophotometer RF-5301 PC, equipped with a constant temperature holder attached to a Neslab RTE-110 water bath with an accuracy of ±0.1 °C. The fluorescence spectra were measured at 25 ± 0.1 °C with a 1 cm path length cell at excitation/emission slit width 5–5 nm. To collect the fluorescence spectra, 5 μM of protein was excited at 295 nm and emission spectra were recorded in the range of 300–400 nm.

2.6. Circular dichroic measurements

CD measurements were carried out on a Jasco spectropolarimeter (J-815) equipped with a Peltier-type temperature controller (PTC-424S/15). The instrument calibration was performed with d-10-camphorsulphonic acid. Spectra were collected in a cell of 1 mm path length with scan speed of 100 nm/min and response time of 1 s for all of the measurements. Each spectrum was the average of 2 scans. The protein concentration was kept 5 μM for far- UV CD.

The raw CD data obtained in millidegrees were converted to mean residue ellipticity (MRE) in deg cm^2 $dmol^{-1}$ which is defined in Eq. (1)

$$\mathrm{MRE} = \frac{\Theta_{obs}(m\ deg)}{10 \times n \times C \times l} \quad (1)$$

where, Θ_{obs} is the CD in millidegrees, n is the number of amino acid residues (686–1 = 685), l is the path length of the cell in cm and C is the molar concentration.

2.7. Thioflavin T fluorescent assay

A stock solution of Thioflavin T (ThT) was prepared in double distilled water. The concentration of ThT was determined using extinction coefficient of (εM) = 36,000 M^{-1} cm^{-1} at 412 nm. Protein samples of 5 μM at different polyols concentration (v/v) were incubated in 1:2 molar ratio of ThT for 30 min at 25 °C. The time for thermal induced aggregation was fixed for 60 min and post heat treatment samples were allowed to cool at room temperature. The method was also repeated for the polyols protected and thermally treated CA. The fluorescence of ThT was excited at 440 nm. The spectra were recorded from 400 to 600 nm. Blanks for ThT was also prepared for GL and EG at increasing concentrations, and was subtracted from the respective samples.

2.8. ANS binding assay

The fresh stock of ANS was prepared in double distilled water, and concentration was determined by using molar extinction coefficient of (εM) = 5000 $M^{-1}cm^{-1}$ at 350 nm. For ANS-binding experiments, the molar ratio of protein to ANS was 1:50. The excitation wavelength was set at 380 nm, and the emission spectra were taken in the range of 400–600 nm. The samples were cooled at room temperature prior to the addition of ANS. Blanks of ANS was prepared for GL and EG at increasing concentrations, and was subtracted from the respective samples.

2.9. Congo red binding assay

The stock solution of Congo red was prepared in double distilled water. The concentration of stock solution was determined using a molar extinction coefficient of 45,000 M^{-1} cm^{-1} at 498 nm. CA (5 μM) was heated at 65 °C for an hour then after cooling the aggregates, sample were further incubated with Congo red (5 μM) for 30 min in the dark. The absorbance spectra of the samples were recorded on a Perkin Elmer (Lambda 25) UV–vis spectrophotometer in a 1 cm path length cuvette and plotted in the range of 400–700 nm.

2.10. Dynamic light scattering (DLS) measurements

The change in aggregation comportment of CA in the different conditions was determined using DLS. For the R_h measurements the protein concentration was taken as 15 μM at 830 nm on a DynaPro–TC–04 dynamic light scattering instrument (Protein Solutions, Wyatt Technology, Santa Barbara, CA) equipped with a temperature controlled microsampler. Prior to the measurements all the solutions were filtered through a 0.22 μm pore sized microfilter (Whatman International, Maidstone, UK). The measured hydrodynamic radius (R_h) was the average of 50 measurements. The mean R_h and polydispersity (Pd) were estimated, on the basis of an autocorrelation analysis of scattered light intensity based on the translational diffusion coefficient, from the Stokes–Einstein Eq. (2)

$$R_h = \frac{kT}{6\pi\eta D_W^{25^\circ C}} \quad (2)$$

where, R_h is the hydrodynamic radius, k is the Boltzmann's constant, T is the absolute temperature, η is the viscosity of water and $D_W^{25^\circ C}$ is the translational diffusion coefficient. All the samples were incubated for 60 min at 65 °C preceding to the measurements.

2.11. Transmission electron microscopy (TEM)

The morphology and size of CA aggregates with and without GL and EG was observed with a JEOL JEM-2100F transmission electron microscope (TEM) with an accelerating voltage of 200 kV. 10 μl of four-fold diluted samples were adsorbed onto copper 400 mesh grid, previously covered by carbon-coated film. After 2 min, excess fluid was drawn out using a paper filter, a drop of 1% uranyl acetate was added and after a few seconds and the samples were observed. A control of native protein solution was also placed on the grids. Images were viewed at 10,000 X.

2.12. Scanning electron microscopy (SEM)

SEM analysis of the surface and cross-section of air dried aliquots of CA aggregate was performed with JSM-6510 LV scanning electron microscope (JEOL, Japan). The aliquots were mounted on carbon tape coated stainless steel grids operating on an accelerating voltage of 15 kV. Gold plating of the aliquots were done for a clearer image. Images were viewed at 5000 X.

3. Results

3.1. Turbidity and Rayleigh light scattering (RLS) measurements

Turbidity measurement is non-specific but a swift and simple method to compare the extent of aggregation in relation to the native protein upon measuring the UV–vis absorbance at 350 nm. The enhanced turbidity cannot directly be correlated with aggregation as the high concentration of protein can show such result. On the other hand, the enhanced turbidity resultant of aggregates do not distinguish the morphology of aggregates *i.e.* amyloid or amorphous, size and nature of aggregate in any case, but it is still sufficiently sensitive to detect the change in magnitude of the presence of sub-visible particles. CA at 25 °C and 37 °C shows negligible turbidity which increases slightly on 45 °C. A significant enhancement in the turbidity has been observed at 55 °C followed by marked augmented turbidity over the temperature range 65–85 °C (Fig. 1A). The increment in the temperature above the 65 °C do not increase turbidity, it is rather slightly decreased for 75 °C and more at temperature 85 °C. The GL and EG protected CA upon increasing concentration (v/v) result in gradual decrease in the turbidity (Fig. 1B–C). Addition of GL in the range of 0–15% (v/v) caused a reduction in turbidity, while EG requires comparatively high concentration 0–35% (v/v) to diminish the turbidity up-to quite effective value.

The analysis of aggregate formation by Rayleigh light scattering (RLS) measurements offer more sensitive approach. Although being more sensitive than turbidity, Rayleigh scattering measurements is still unable to differentiate the morphology of aggregates in accordance of amyloid of amorphous.

The light scattering and turbidometric measurements of thermally challenged CA shows similar pattern. The initial increment in the temperature (25–37 °C), do not cause any significant scattering,

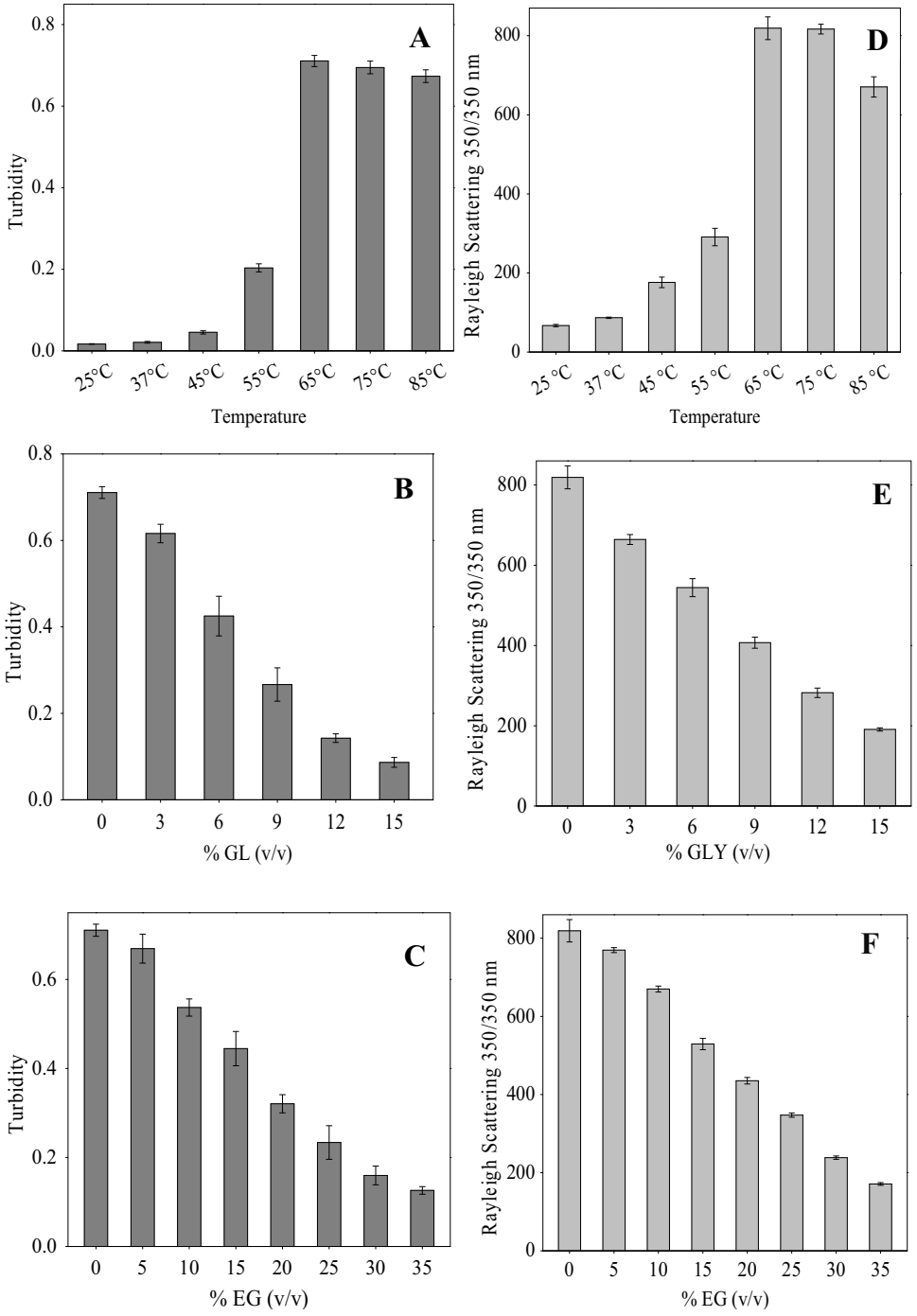

Fig. 1. Turbidity measurements of CA at 350 nm at (A) increasing temperature (25–85 °C), at (B) increasing concentration of GL from 3 to 15% (v/v), and (C) increasing concentration of EG from 5 to 35% (v/v). Rayleigh measurements of CA at 350/350 nm at (D) increasing temperature (25–85 °C), at (E) increasing concentration of GL from 3 to 15% (v/v), and (F) increasing concentration of EG from 5 to 35% (v/v). Error bars represent the mean ± SD ($n = 3$).

while the significant enhancement in the scattering begins from 45 °C which reaches maximum values at 65 °C. Further increase in the temperature causes minor decrease in the scattering (Fig. 1D). The incubated CA with GL and EG demonstrate the continuous decrease in Rayleigh scattering. Addition of GL concentration of 3% (v/v), followed by addition of further GL up to 15% (v/v) show a gradual decline in scattering (Fig. 1E). The addition of EG also produce the same effect (Fig. 1F), and lead to a decrease in the scattering upon increasing the concentration from 5 to 35% (v/v).

3.2. Tryptophan fluorescence measurements

The microenvironment of Trp of CA, a deca Trp containing protein [38], was investigated by Trp fluorescence study upon thermal treatment and increasing concentration of polyols at 65 °C. In native condition Trp residues are present in the hydrophobic core [39]. Unfolding of protein (during heating) causes a red shift (from 331 to 340 nm), (Fig. 2A) that connote the replacement of Trp residues from less polar towards more polar interior [40]. The addition of GL (15%) and EG (35%) cause blue shift (from 337 to 332 nm),

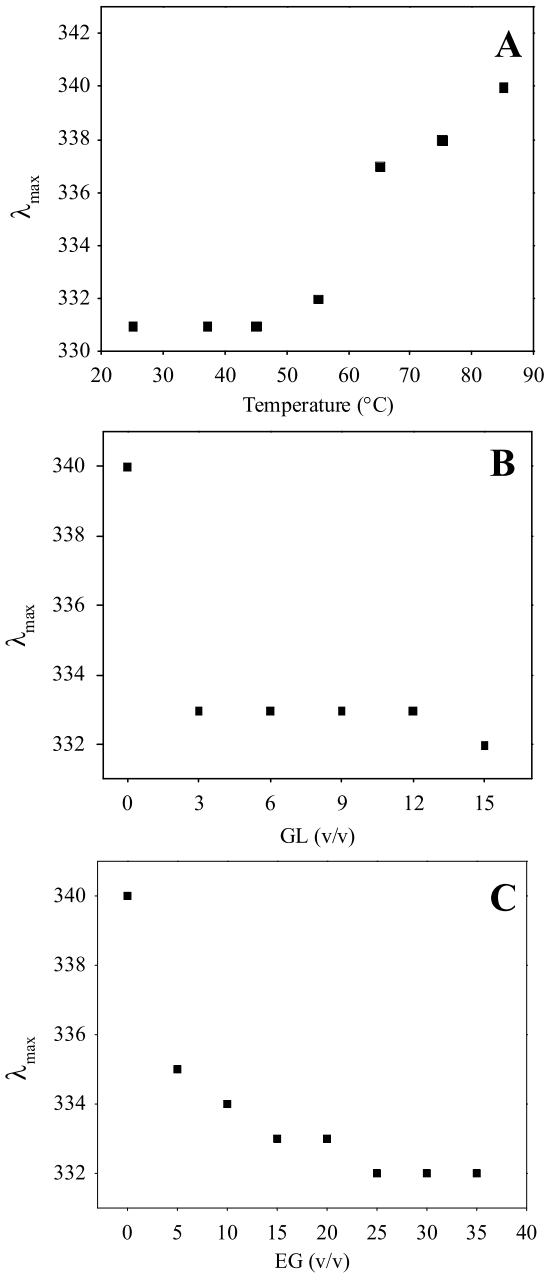

Fig. 2. The change in the microenvironment of Trp of CA: at (A) increasing the temperature from 25 to 85 °C, at (B) increasing concentration of GL3-15% (v/v) and (C) increasing concentration of EG 5–35% (v/v) at 65 °C.

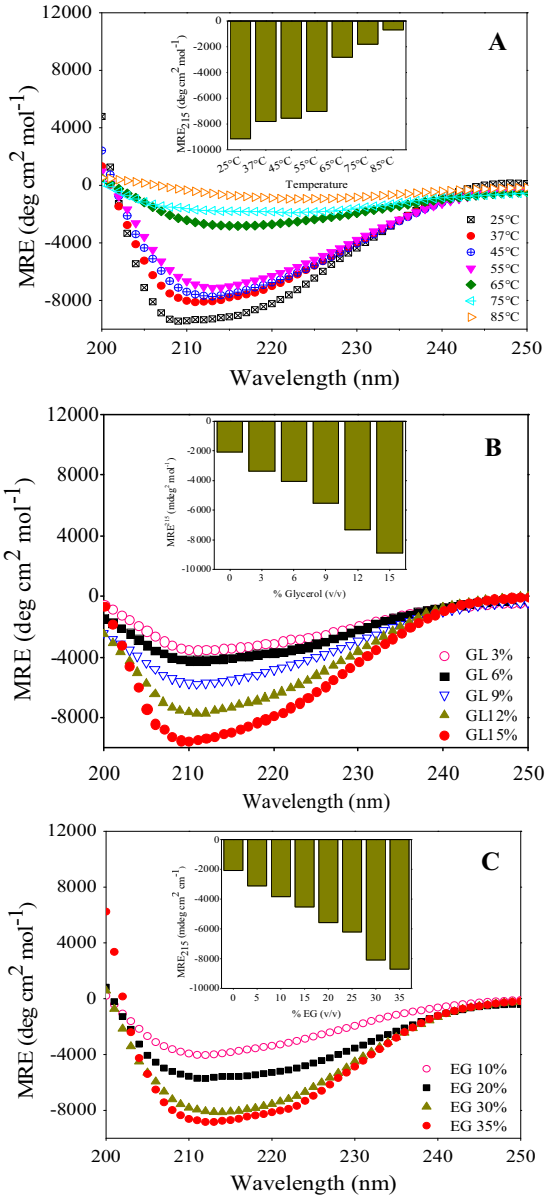

Fig. 3. Effect of various conditions on the secondary structure of CA: (A) Far-UV CD spectra of CA on increasing the temperature from 25 to 85 °C. (B) Gradual induction in secondary structure and conformational restoration at 65 °C for 60 min heat treatment, on increasing concentration of GL3-15% (v/v) and (C) EG 5–35% (v/v).

(Fig. 2B–C) suggesting the arrangement of Trp residue towards the more hydrophobic environment and this data is compatible with reported study [41].

3.3. Circular dichroic (CD) measurements

Temperature induced conformational adaptation and interceding of secondary structure upon the addition of polyols was studied using far-UV CD spectroscopy since this technique is specific for the determination of proteins secondary structures [39,42–44]. The native CA exhibits two negative minima at 208 and 222 nm, which slightly get disturbed at 37 °C, (Fig. 3A). The further temperature elevation up to 55 °C leads the major change in the conformation, depicted by lowering the ellipticity and shifting of two characteristic negative minima to single trough. The next set of temperature *i.e.* at 65 °C, the most sweeping consequence (% ΔMRE_{215} = 69) has been observed which show a single trough concentrated at 215 nm followed by much significant lowering in intensity compared to the previous set of temperature (Table 1).We have examined the outcome of the temperature increase within the range of 75–85 °C and detected very less amount of secondary structure % ΔMRE_{215} = 80 for 75 °C and 93 for 85 °C respectively, with great loss in signal on equating with native CA. During the temperature increase, the loss in MRE_{215nm} continuously increased (Fig. 3A inset).

The augmentation of CD signals and transformation of single trough into two negative minima at 208 and 222 nm was investigated by the addition of initial GL concentration, 3% (v/v). The effect of GL continues in accordance with the gradual increase and nearly native-like secondary structure (Fig. 3B) was restored by final addition used, 15% (v/v). A similar stabilizing behavior of polyols has been established by gradual increase in the EG concentration added to CA. The lowest EG concentration of 5% (v/v) efficiently shields

Table 1
Spectroscopic parameters and Hydrodynamic radii (R_h), *App.* M.W. and other parameters of native CA (pH 7.0, room temperature), in aggregated condition at 65 °C, pre-incubated with GL 15% (v/v) and EG 35 (v/v).

Properties	Native	CA at 65 °C	GL 6% (v/v)	GL15% (v/v)	EG 15% (v/v)	EG 35% (v/v)
Turbidity	0.016	0.71	0.42	0.08	0.44	0.08
R. scattering	67	819	544	191	529	171
Trp λ_{max} λ_{max} (nm)	331	337	333	332	333	332
MRE_{208nm}	−9311	−2080	−3971	−9263	−4306	−7984
MRE_{215nm}	−9146	−2814	−4043	−8894	−4525	−8703
MRE_{222nm}	−7624	−2580	−3511	−7294	−3749	−7898
ΔMRE_{208nm} (%)	–	−77	−57	−0.5	−54	−14
ΔMRE_{215nm} (%)	–	−69	−56	−3.0	−50	−5.0
ΔMRE_{222nm} (%)	–	−66	−54	−4	−50	+3.0
$\Theta_{222}/\Theta_{208}$	0.8	1.2	0.8	0.7	0.8	0.9
ThT FI FI 480 (nm) ***ANS FI***	9	169	91	20	87	28
FI 480 (nm)	27	337	311	126	223	105
λ_{max} (nm)	472	480	469	469	466	468
R_h [nm]	5.1	103	–	5.4	–	5.6
App. M.W. [kDa]	152	431541	–	192	–	214
P_d[%]	13	26	–	18	–	19

CA during thermal treatment and further addition of EG fortify this protective effect. During the stabilization of CA from thermal treatment, the final concentration of EG added, 35% was found to be sufficient to achieve native like spectra showing two negative minima with good ellipticity (Fig. 3C). The % ΔMRE_{215} for GL15% (v/v) and EG 35% (v/v) was found to be −3 and −5 (Table 1), as shown in the plot (Fig. 3B–C inset). The time dependent CD spectra of CA in presence of glycerol and EG reveal that restoration of secondary structure after 1 h was similar to the native one and restoration was constant up to 24 h that indicates the inhibition of CA aggregation in presence of polyols. The CD spectra of denatured state of CA at 75 °C and incubation up to 24 h show there is no re-naturation occurs of the denatured protein (Supplementary data 1).

3.4. Thioflavin T (ThT), ANS (1-anilinonaphtalene 8-sulfonic acid) and Congo red (CR) fluorescent assay

The fluorescent dye, ThT is specific to detect the presence of cross β sheet formed due to the formation of amyloid fibrils in tissues as well as in the *in vitro* samples. Following its interaction with amyloid fibrils, ThT shows greatly enhanced emission spectra near 480 nm compared to the native protein, while showing very low interaction followed by negligible emission spectra for the amorphous aggregates [22,45]. Elevated temperature dictates the alteration in conformation of CA. The native CA which do not show significant emission spectra at 25 °C, show slight increment at 55 °C. During heat treatment, the most significant emission spectra is produced at 65 °C which is nearly 19 times higher than the native, whereas, further temperature elevation brings the decline of ThT spectra (Fig. 4A), (Table 1).

The pre-incubation of GL and EG with CA followed by 1 h heat treatment at 65 °C, show inhibitory effect on ThT fluorescence intensity. The addition of GL on increasing concentration from 3 to 15% (v/v) and EG from 5 to 35% (v/v) resulted in a decrease in the fluorescence intensity (Fig. 4B–C). The protein incubated with GL 15% (v/v) and EG 35% (v/v) exhibits lowering of ThT fluorescence intensity and remains merely 5 and 7 times more than native respectively, (Table. 1).

ANS access the extent of exposure of hydrophobic cluster in accordance with solvent, present on the protein surface which progressively changes in the protein destabilization conditions [46]. The native protein has a minimum exposure of hydrophobic cluster to the solvent and produce very low intensity upon its excitation at 380 nm. Following its exposure to more heat, CA unfolds and the level of exposure increases up to the 65 °C, at which protein undergoes unfolding followed by polymerization and within 1 h CA gets aggregated and fluorescence intensity is enhanced by ∼13 fold than native (Table 1). At the temperature range 75–85 °C, the ANS shows a decrease in the fluorescence intensity but the intensity remains significant (Fig. 4D). The addition of polyols decreases the ANS fluorescence intensity as a function of increasing concentration by mediating the protein stabilization and regulating the exposure of hydrophobic patches (Fig. 4E–F). At the highest added concentrations of GL 15% (v/v) and EG 35% (v/v), the slightly significant signals of ANS fluorescence suggest the presence of some little hydrophobic pockets on the surface of the induced secondary structure which provide site for ANS interaction (supplementary Fig. S2), (Table 1). It was also observed that the ANS itself strongly interacts with both of the polyols and its fluorescence intensity is enhanced as the concentration of GL and EG are increased (data not shown), so the resulting effect of the polyols addition on the exposed hydrophobic patches was obtained by subtracting the blank.

The nature of the CA aggregate formed at 65 °C was further investigated by Congo red (CR) to further investigate whether the aggregates are amorphous or amyloid. Congo red shows an intercalation property and places itself in the fissure of the cross β-sheets which came into existence at the event of amyloid fibrils followed by red shift in the absorption spectrum [47]. The CA aggregates upon its incubation with CR in 1:2 molar ratio for 30 min producing maximum absorption at 497 nm.CA with GL15% (v/v) and EG 35% (v/v), show maximum absorption at 496 nm along with much significant reduction in the absorption intensity (supplementary Fig. S3). The insignificant shift in the absorption spectra with high absorption intensity confirms the existence of amorphous aggregates, while significant reduction in the absorption intensity corroborates the absence of such aggregate population.

3.5. Dynamic light scattering (DLS) measurements

The DLS is used for the determination and analysis of proteins particle size as well as to distinguish the protein aggregates in the sample. The hydrodynamic radii (R_h) of the native CA (neutral pH), aggregates formed during heat treatment, GL 15% (V/V) and EG 35% (v/v) protected protein were all studied by DLS. The R_h of CA at neutral pH was observed to be 5.1 nm (Fig. 5A), which is compatible with reported value [39], but it drastically increased to be 103 nm at 65 °C (Fig. 5B), confirming that the CA has undergone aggregation followed by polymerization. The heat treatment prior to the GL 15% (v/v) and EG 35% (v/v) pre-incubation, managed to keep the CA in its monomeric form and the R_h was found to be 5.4 and 5.6, respectively (Fig. 5C–D), which is slightly greater than its native value. The recapitulation of observation obtained by Table 1 indicate the reversal of nearly overall conformation of polyols protected CA.

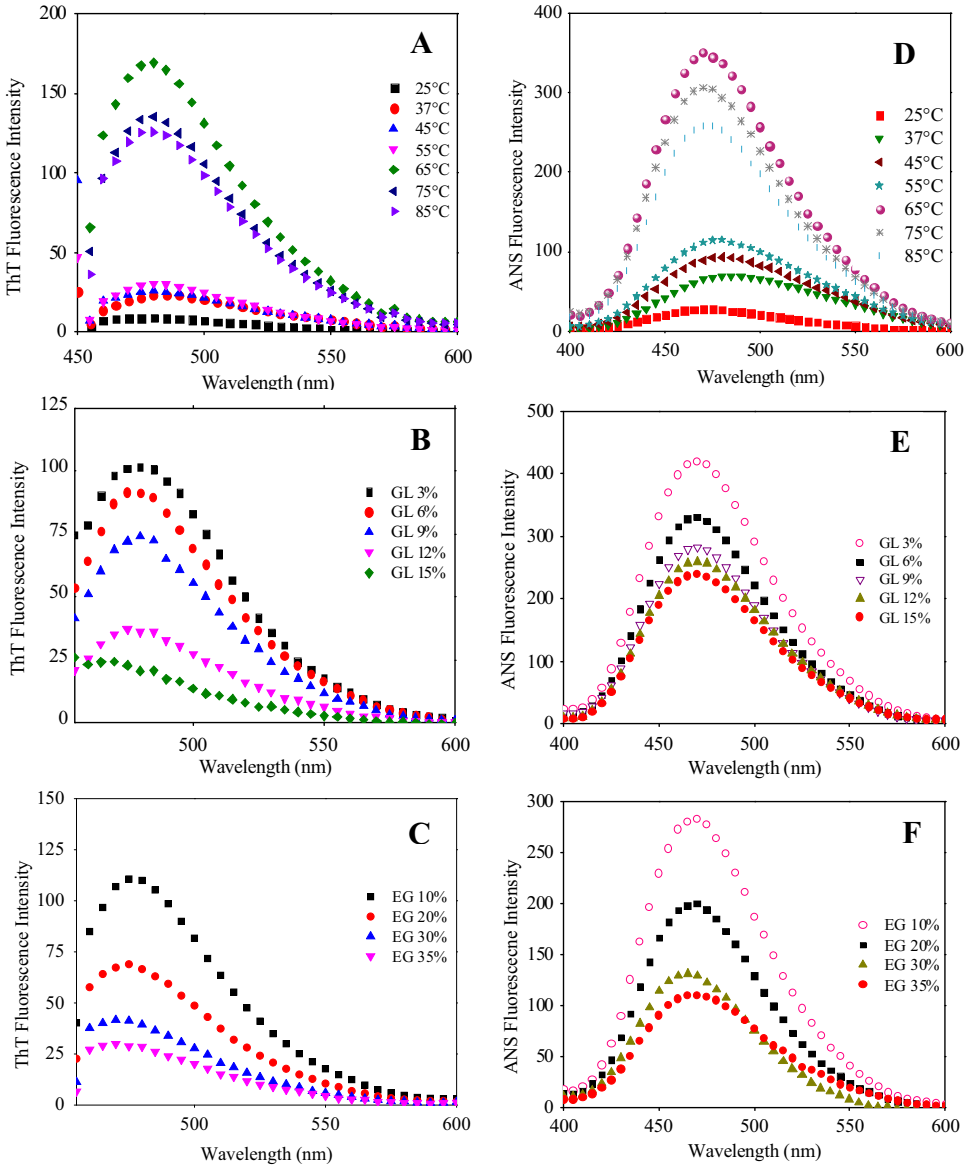

Fig. 4. Effect of various conditions on the ThT-fluorescence intensity: (A) increase in ThT-fluorescence intensity from 25 to 65 °C and decrease in ThT-fluorescence intensity from 75 to 85 °C. (B) Reduction in ThT-fluorescence intensity on addition of GL3-15% (v/v) and (C) on addition of EG 5–35% (v/v). Change in ANS-fluorescence intensity on varying the condition: (D) increase in ANS-fluorescence intensity as the temperature rise from 25 to 65 °C and decrease in ANS-fluorescence intensity in the temperature range of 75–85 °C. (E) The continuous reduction in ANS-fluorescence intensity on addition of GL3-15% (v/v) and (F) on addition of EG 5–35% (v/v) at 65 °C.

3.6. Transmission and Scanning electron microscopy (TEM and SEM) analysis

For a more detailed investigation of the morphology of CA upon aggregation and inhibition by GL and EG, the resulting TEM images were examined. The TEM image analysis reveals the morphological appearance which clearly distinguishes existence of the type of aggregates of proteins including CA. As expected the native CA do not show any morphological appearance (Fig. 6A) while CA at 65 °C show aggregates (Fig. 6B) which lacks any fibrillar structure, that is consistent with previously published reports [22,45]. The sample containing polyols, GL 15% (v/v) and EG 35% (v/v) protects the CA from forming any aggregates (Fig. 6C–D). The TEM imaging data is consistent with the data obtained by CD, ANS and CR results.

The SEM imaging also evidence the absence of any morphological appearance of native CA (Fig. 6E) and presence of non-fibrillar structure of protein sample treated at 65 °C (Fig. 6F).The sample containing GL 15% (v/v) and EG 35% (v/v), show image proving that the polyols are restricting the CA monomer to form aggregates and give clear image (Fig. 6G–H).

4. Discussion

Glycerol and ethylene glycol both shares common properties like they are osmolytes, polyols and cryoprotectant. However, GL, by showing chemical chaperon activity, supersedes the fellow additive. Both the GL and EG strongly interact with the native, acid denatured and thermal denatured conformation of glucoamylase (GA) of *Aspergillus niger*. Glycerol shows more enhancement in CD signal (at $MRE_{222\,nm}$) than EG at the same concentration. The condition is different for the thermal denatured protein where EG destabilize the protein and CD signal decreases while glycerol still maintains the conformation integrity by giving more CD signal compared to the native [41].

Acting as a chemical chaperon, glycerol (7 M) surpasses the molecular chaperon (GroEL and GroES) *in vitro* in terms of total

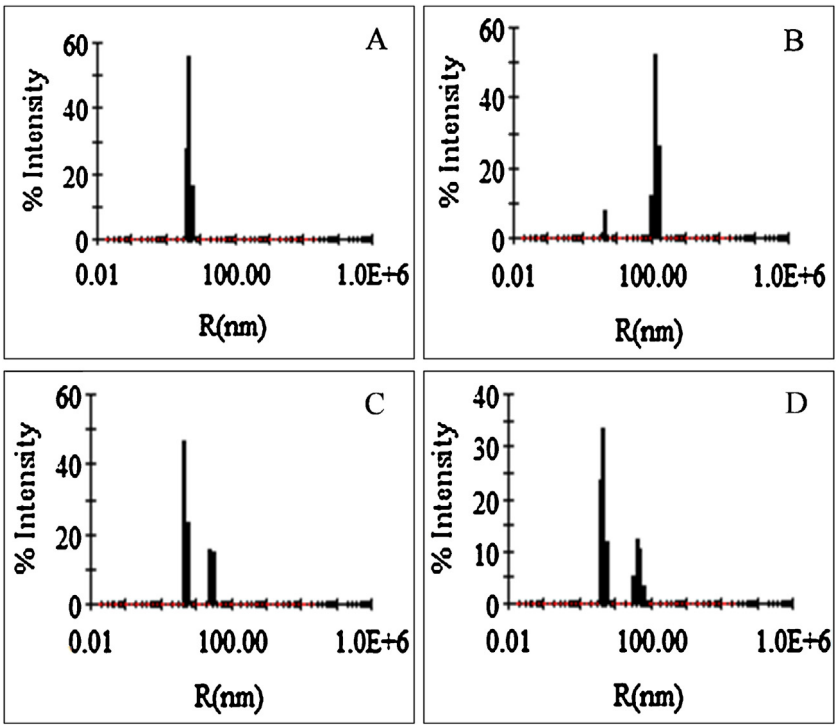

Fig. 5. Hydrodynamic radii (R_h) were measured to know the size of aggregates. The hydrodynamic radii (R_h) of (A) native CA at 15 μM, at (B) 65 °C, (C) in the presence GL15% (v/v) and (D) EG 35% (v/v).

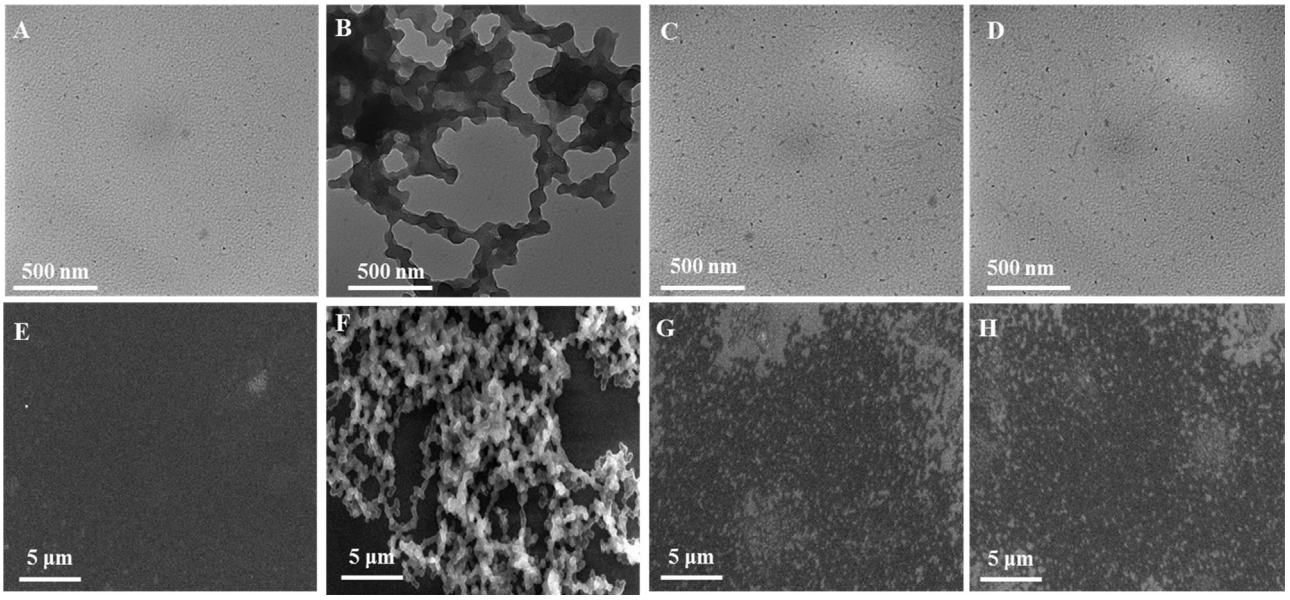

Fig. 6. Morphology of aggregate was detected by Transmission electron microscope (TEM). TEM images of CA (5 μM) at (A) 25 °C, at (B) 65 °C, at (C) GL15% (v/v) and at (D) EG 35% (v/v). Morphology of aggregate was detected by Scanning electron microscope (SEM). SEM images of CA (5 μM) at (E) 65 °C, at (F) 65 °C, at (G) GL5% (v/v) and at (H) EG 35% (v/v).

enzymatic recovery of citrate synthase during refolding. The inactivation kinetics study of citrate synthase revealed that loss of complete activity is a consequence of high temperature (45 °C) for an incubated period of 25 min, but the native conformation and 20% enzymatic activity was resorted on addition of 7 M glycerol [48].

The effect of osmolytes mimicking as molecular crowder cannot be generalize for the proteins, as it destabilize the aggregates but also destabilize the partially unfolded state and alter the amyloidosis by extending the lag time [31,49,50]. Moreover, modulation of osmolytes concentration produce tremendous effect of disaggregation of preformed aggregates as well as conversion of insoluble precipitates in to soluble aggregates [51]. Cosolutes also govern the refolding of protein which differs significantly for the reduced and oxidized state. The solute push the reduced state in towards the aggregation resulting decline in the refolding yield [52].

Moreover, the turbidity and RLS scattering is maximum at 65 °C, but in range of 75–85 °C, the cloudiness (Fig. 1A and D) with slight low turbidity and scattering indicate that protein denatures and the onset of aggregation occurs just before the denaturation. The same pattern was also observed at neutral pH (close to isoelectric point)

as denaturation occurs in the pI range of CA 6.0-6.8 [53]. The reduction in turbidity and Rayleigh scattering is due to the interaction of polyols with CA which nearly quash the impact of heat treatment. The change in λ_{max} was investigated to evaluate the refolding or unfolding of CA when processed during the experimental condition. We observed the neutrality of temperature range 25–45 °C on the λ_{max}, while above this, a dramatic change with red shift of 9 nm was observed. The movement of Trp residues toward more hydrophobic region was accompanied by blue shift of 5 nm, when CA was incubated with increasing concentration of GL and EG.

CA at increasing temperature showed gradual decrease in the CD signal due to conformation alteration caused by heat. The unique single trough was obtained at 65 °C due to the aggregate formation while elevation in temperature beyond this point causes denaturation of protein and loss of signal, (Fig. 3A). The steady conformational restoration was shown by both the polyols upon increasing the concentration, accompanied by addition of final concentration of GL 15% (v/v) and EG 35% (v/v) which restores nearly overall secondary structure detected by CD measurements (Fig. 3B–C). The induction in the secondary structure has also been observed in reduced lysozyme on the addition of EG. Increasing the concentration of EG (0–40%), enhanced the value of negative ellipticity of single peak focused around the 218 nm through refolding. The induced secondary structure of refolded lysozyme by ethyl alcohol lacks α-helical conformation and is not comparable with the native state but showed higher magnitude of activity than reduced state [54].

Binding of ThT cause significant augmentation in fluorescence intensity (Fig. 4A) on CA aggregate binding which directly opposite to the result obtained by ANS, CR, TEM and SEM. This might be possible due to formation cross-β sheet in amorphous aggregates [55] of CA but ANS data contradict the result by showing comparatively high ANS emission for amorphous than amyloid [22,45]. The CD data depict the conformational restoration of the overall secondary structure of CA at GL15% (v/v) and EG 35% (v/v), but substantial amount of ANS fluorescence was also observed. The reason behind the remarkable ANS fluorescence is not due to exposed hydrophobic patches of CA protected by GL and EG, rather GL shows high binding affinity (Fig. 4E–F, Supplementary Fig. S2) with ANS and competes for the interaction [56], probably this is also true in case of EG.

Comparing the ANS data for amorphous and amyloid aggregates further confirms that the aggregates are amorphous in nature. Some scientists have reported such non-specific interaction of ThT with non-amyloidal fibrils [57]. Even in more astonishing condition, listeria O (LLO), a toxin produced by *Listeria monocytogenes,* a gram-positive bacterium, gets aggregated at pH 7.5 but gives a positive response for both amyloid specific dye ThT and CR while TEM images confirm the presence of unordered, non-fibrillar, amorphous aggregates [58]. The substantial enhancement in ThT fluorescence intensity and shifting in CR absorption spectra (supplementary Fig. S3) upon binding with amorphous aggregates suggest the possibility of successful stacking of ThT molecule in the crevices generated by aggregation.

Binding of the CA aggregates with CR do not lead the shift in absorption rather the optical density of absorption spectra increase which also is suggestive of the presence of amorphous aggregates. Similarly, the pre-incubated CA with GL and EG, decrease the Congo red spectra (supplementary Fig. S3). The DLS data divulge the difference of hydrodynamic radii (R_h) of aggregated CA which is nearly 20 times (103 nm) than native (5.1). GL 15% (v/v) and EG 35% (v/v) preserves CA at monomeric form even at 65 °C and prevent oligomerization (Fig. 5) but interaction of CA with polyols slightly increase the hydrodynamic radii (R_h) as well as apparent molecular weight (Table 1). The collective consideration of all data obtained, GL is found to be more effective than EG. The effect produced by EG for the conformational restoration of CA is achieved by the addition of nearly half of the concentration of GL. The ability of ethylene glycol for weakening the hydrophobic interaction amid sorbent and protein, serves itself as admirable mobile phase for the protein purification method involving hydrophobic interaction chromatography [59]. In which, ethylene glycol serves itself as excellent mobile phase by declining the hydrophobic interaction between sorbent and protein molecule.

Several models have been proposed to explain the mechanism and pathways of aggregate formation, but in case of CA it is following the mechanism of aggregation in conformational altered monomer serves as aggregation precursor. In this mechanism monomer, primarily with low proclivity of reversible association, undergoes conformation transformation *via* unfolding which enables the strong association under physical strain. The thermal stress cause the destabilization of CA and the unfolded state followed by display of hydrophobic patches which allow the hydrophobic-hydrophobic interaction for finally aggregation. For the protection of CA conformation and anti-aggregation activity, the protection of CA monomer is a prerequisite. The pre-incubation of CA with GL 15% (v/v) and EG 35% (v/v), allows their interaction with CA monomers and hamper the thermal stress to produce unfolded population, hence, unavailability of such unfolded precursor cannot lead the aggregation (Fig. 7).

The excluded volume model explain that crowding influence the equilibrium of macromolecular reaction by either accelerating or retarding the compaction but the effect strictly depend on the compaction of initial conformation [60]. The osmolytes mediated stabilization of protein depend on the osmolytes-water interaction as double resolution model suggest that TMAO interact with two or three water molecule which prohibit the closeness of TAMO with protein *via* exclusion from the locality of protein [61]. The exact mechanism of structural modulation triggered by addition of cosolutes remains ambiguous, although adequate works are available, proposing various models like, enhanced surface tension, Wyman binding function, preferential hydration, and excluded volume [62,63]. Increases in polyols concentration modulate the hydrophobic patches by pushing them towards the interior of proteins which causes compactness in proteins. Further, this compactness of protein hinder the hydrophobic-hydrophobic interaction (the main culprit of aggregation of protein) and thus inhibition of protein occurs as reported in previous literatures [64,65].

5. Conclusion

This study demonstrates that the polyols (GL and EG) are successfully able to inhibit the temperature mediated amorphous aggregation and induce native like conformation. Our results have also extended the example in exception of such protein which shows significant ThT binding even with amorphous aggregates. The little expansion in the radius but condense the core size of conalbumin occurs upon the interaction with GL and EG. For the overall conformational restoration, GL was found to be more effective than EG as it requires 15% (v/v) as compared to EG 35% (v/v). It would be very significant in future studies to investigate how polyols are further affecting the activity of pre-incubated proteins on thermal or other destabilizing stress. In case of successful restoration of enzymatic activity of proteins upon the addition of low concentrations of polyols will provide excellent lead against the harsh conditions encountered by protein in industries as well as transportation. The inhibition is due to hindrance of hydrophobic interaction (responsible for aggregation) that is caused by compactness of proteins as a result of shifting of hydrophobic patches in the inner side of proteins. Further, glycerol due to its hydrophobic

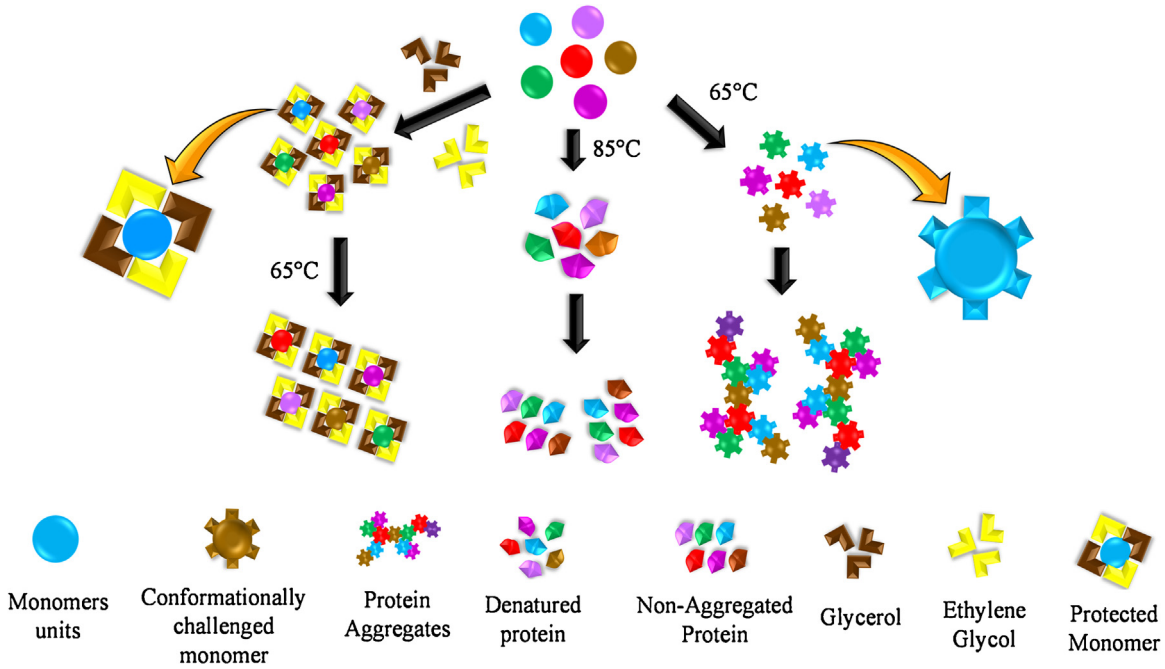

Fig. 7. Schematic representation of conformational alteration of CA, showing aggregate formation at 65 °C while denaturation at beyond this temperature range. Cartoon illustrate the inhibition of CA aggregates at 65 °C by the addition and incubation of GL15% (v/v) and EG 35% (v/v) through stabilization of monomeric CA which resist thermal impact from unfolding and further aggregation.

nature also competes for the hydrophobic patches on the proteins and affects the hydrophobic interactions.

Competing financial interests

Authors declare no competing financial interest.

Acknowledgements

Mohsin Vahid Khan would like to thanks University Grant Commission (UGC), New Delhi for providing financial assistance in the form of JRF as Basic Scientific Research (BSR) fellow. The authors would also like to thank the Interdisciplinary Biotechnology Unit, for providing instrumental facilities and University Sophisticated Instruments Facility (USIF), Aligarh Muslim University for providing the facility for TEM and SEM. The authors extend their appreciation to the International Scientific Partnership Program ISPP at King Saud University for funding the research work through ISPP# 0014.

Appendix A. Supplementary data

Supplementary data associated with this article can be found, in the online version, at http://dx.doi.org/10.1016/j.ijbiomac.2016.10.023.

References

[1] C.M. Dobson, The structural basis of protein folding and its links with human disease, Philos. Trans. R Soc. Lond. B Biol. Sci. 356 (2001) 133–145.
[2] R.J. Ellis, T.J. Pinheiro, Medicine: danger–misfolding proteins, Nature 416 (2002) 483–484.
[3] R. Jaenicke, Protein self-organization in vitro and in vivo: partitioning between physical biochemistry and cell biology, Biol. Chem. 379 (1998) 237–243.
[4] V. Militello, V. Vetri, M. Leone, Conformational changes involved in thermal aggregation processes of bovine serum albumin, Biophys. Chem. 105 (2003) 133–141.
[5] R.J. Truscott, Age-related nuclear cataract-oxidation is the key, Exp. Eye Res. 80 (2005) 709–725.
[6] G. Gallo, M. Picken, J. Buxbaum, B. Frangione, The spectrum of monoclonal immunoglobulin deposition disease associated with immunocytic dyscrasias, Semin. Hematol. 26 (1989) 234–245.
[7] D. Ganeval, L.H. Noel, J.L. Preud'homme, D. Droz, J.P. Grunfeld, Light-chain deposition disease: its relation with AL-type amyloidosis, Kidney Int. 26 (1984) 1–9.
[8] S.Y. Tan, M.B. Pepys, Amyloidosis, Histopathology 25 (1994) 403–414.
[9] S. Ventura, Sequence determinants of protein aggregation: tools to increase protein solubility, Microb. Cell Fact. 4 (2005) 11.
[10] B.A. Chrunyk, J. Evans, J. Lillquist, P. Young, R. Wetzel, Inclusion body formation and protein stability in sequence variants of interleukin-1 beta, J. Biol. Chem. 268 (1993) 18053–18061.
[11] G.A.E.J. Waters, R. Muhlack, K.F. Pocock, B.K.O.N.C. Colby, a.P.J.P.B. HØJ, Preventing protein haze in bottled white wine, Aust. J. Grape Wine Res. 11 (2005) 215–225.
[12] T.B. Eronina, N.A. Chebotareva, S.G. Roman, S.Y. Kleymenov, V.F. Makeeva, N.B. Poliansky, K.O. Muranov, B.I. Kurganov, Thermal denaturation and aggregation of apoform of glycogen phosphorylase b. Effect of crowding agents and chaperones, Biopolymers 101 (2013) 504–516.
[13] S. Swamy-Mruthinti, V. Srinivas, J.E. Hansen, M. Rao Ch, Thermal stress induced aggregation of aquaporin 0 (AQP0) and protection by alpha-crystallin via its chaperone function, PLoS One 8 (2013) e80404.
[14] Y.B. Yan, Q. Wang, H.W. He, H.M. Zhou, Protein thermal aggregation involves distinct regions: sequential events in the heat-induced unfolding and aggregation of hemoglobin, Biophys. J. 86 (2004) 1682–1690.
[15] F. Salmannejad, N. Nafissi-Varcheh, A. Shafaati, R. Aboofazeli, Study on the effect of solution conditions on heat induced-aggregation of human alpha interferon, Iran J. Pharm. Res. 13 (2014) 27–34.
[16] Y.N. Lee, L.K. Chen, H.C. Ma, H.H. Yang, H.P. Li, S.Y. Lo, Thermal aggregation of SARS-CoV membrane protein, J. Virol. Methods 129 (2005) 152–161.
[17] Y. Yoshimura, Y. Lin, H. Yagi, Y.H. Lee, H. Kitayama, K. Sakurai, M. So, H. Ogi, H. Naiki, Y. Goto, Distinguishing crystal-like amyloid fibrils and glass-like amorphous aggregates from their kinetics of formation, Proc. Natl. Acad. Sci. U. S. A. 109 (2012) 14446–14451.
[18] V. Vetri, C. Canale, A. Relini, F. Librizzi, V. Militello, A. Gliozzi, M. Leone, Amyloid fibrils formation and amorphous aggregation in concanavalin A, Biophys. Chem. 125 (2007) 184–190.
[19] J. Goers, S.E. Permyakov, E.A. Permyakov, V.N. Uversky, A.L. Fink, Conformational prerequisites for alpha-lactalbumin fibrillation, Biochemistry 41 (2002) 12546–12551.
[20] J. Nieva, A. Shafton, L.J. Altobell 3rd, S. Tripuraneni, J.K. Rogel, A.D. Wentworth, R.A. Lerner, P. Wentworth Jr., Lipid-derived aldehydes accelerate light chain amyloid and amorphous aggregation, Biochemistry 47 (2008) 7695–7705.
[21] M. Ishtikhar, T.I. Chandel, A. Ahmad, M.S. Ali, H.A. Al-Lohadan, A.M. Atta, R.H. Khan, Rosin surfactant QRMAE can be utilized as an amorphous aggregate

inducer: a case study of mammalian serum albumin, PLoS One 10 (2015) e0139027.
[22] M.V. Khan, G. Rabbani, M. Ishtikhar, S. Khan, G. Saini, R.H. Khan, Non-fluorinated cosolvents: a potent amorphous aggregate inducer of metalloproteinase-conalbumin (ovotransferrin), Int. J. Biol. Macromol. 78 (2015) 417–428.
[23] M. Zaman, S.M. Zakariya, S. Nusrat, M.V. Khan, A. Qadeer, M.R. Ajmal, R.H. Khan, Surfactant-mediated amyloidogenesis behavior of stem bromelain; a biophysical insight, J. Biomol. Struct. Dyn. (2016) 1–13.
[24] M. Beland, M. Bedard, G. Tremblay, P. Lavigne, X. Roucou, Abeta induces its own prion protein N-terminal fragment (PrPN1)-mediated neutralization in amorphous aggregates, Neurobiol. Aging 35 (2014) 1537–1548.
[25] J.B. Wang, Y.M. Wang, C.M. Zeng, Quercetin inhibits amyloid fibrillation of bovine insulin and destabilizes preformed fibrils, Biochem. Biophys. Res. Commun. 415 (2011) 675–679.
[26] M.R. Ajmal, S.K. Chaturvedi, N. Zaidi, P. Alam, M. Zaman, M.K. Siddiqi, S. Nusrat, M.S. Jamal, M.H. Mahmoud, G. Badr, R.H. Khan, Biophysical insights into the interaction of hen egg white lysozyme with therapeutic dye clofazimine: modulation of activity and SDS induced aggregation of model protein, J. Biomol. Struct. Dyn. (2016) 1–14.
[27] S. Khan, M. Adnan, S. Haque, M. Lohani, M. Khan, C.K. Tripathi, A modified Lumry-Eyring analysis for the determination of the predominant mechanism underlying the diminution of protein aggregation by glycerol, Cell Biochem. Biophys. 68 (2014) 133–142.
[28] C.R. Lowe, K. Mosbach, Biospecific affinity chromatography in aqueous-organic cosolvent mixtures. The effect of ethylene glycol on the binding of lactate dehydrogenase to an immobilised-AMP analogue, Eur. J. Biochem. 52 (1975) 99–105.
[29] H. Muller, L. Stitz, H. Wille, S.B. Prusiner, D. Riesner, Influence of water, fat, and glycerol on the mechanism of thermal prion inactivation, J. Biol. Chem. 282 (2007) 35855–35867.
[30] Y. Gu, N. Singh, Doxycycline and protein folding agents rescue the abnormal phenotype of familial CJD H187R in a cell model, Brain Res. Mol. Brain Res. 123 (2004) 37–44.
[31] S. Sukenik, R. Politi, L. Ziserman, D. Danino, A. Friedler, D. Harries, Crowding alone cannot account for cosolute effect on amyloid aggregation, PLoS One 6 (2011) e15608.
[32] P. Aisen, I. Listowsky, Iron transport and storage proteins, Annu. Rev. Biochem 49 (1980) 357–393.
[33] P. Valenti, G. Antonini, C. Von Hunolstein, P. Visca, N. Orsi, E. Antonini, Studies of the antimicrobial activity of ovotransferrin, Int. J. Tissue React. 5 (1983) 97–105.
[34] F. Giansanti, M.T. Massucci, M.F. Giardi, F. Nozza, E. Pulsinelli, C. Nicolini, D. Botti, G. Antonini, Antiviral activity of ovotransferrin derived peptides, Biochem. Biophys. Res. Commun. 331 (2005) 69–73.
[35] H. Xie, L. Newberry, F.D. Clark, W.E. Huff, G.R. Huff, J.M. Balog, N.C. Rath, Changes in serum ovotransferrin levels in chickens with experimentally induced inflammation and diseases, Avian Dis. 46 (2002) 122–131.
[36] H.R. Ibrahim, M.I. Hoq, T. Aoki, Ovotransferrin possesses SOD-like superoxide anion scavenging activity that is promoted by copper and manganese binding, Int. J. Biol. Macromol. 41 (2007) 631–640.
[37] H.R. Ibrahim, T. Kiyono, Novel anticancer activity of the autocleaved ovotransferrin against human colon and breast cancer cells, J. Agric. Food Chem. 57 (2009) 11383–11390.
[38] R.E. Feeney, S.K. Komatsu, The Transferrins Structure and Bonding, 1, 1966, pp. 149–206.
[39] G. Rabbani, E. Ahmad, N. Zaidi, R.H. Khan, pH-dependent conformational transitions in conalbumin (ovotransferrin), a metalloproteinase from hen egg white, Cell Biochem. Biophys. 61 (2011) 551–560.
[40] C. Duy, J. Fitter, How aggregation and conformational scrambling of unfolded states govern fluorescence emission spectra, Biophys. J. 90 (2006) 3704–3711.
[41] M.S. Zaroog, H. Abdul Kadir, S. Tayyab, Stabilizing effect of various polyols on the native and the denatured states of glucoamylase, Sci.World J. 2013 (2013) 570859.
[42] M. Ishtikhar, M.V. Khan, S. Khan, S.K. Chaturvedi, G. Badr, M.H. Mahmoud, R.H. Khan, Biophysical and molecular docking insight into interaction mechanism and thermal stability of human serum albumin isoforms with a semi-synthetic water-soluble camptothecin analog irinotecan hydrochloride, J. Biomol. Struct. Dyn. 34 (2016) 1545–1560.
[43] M.R. Ajmal, N. Zaidi, P. Alam, S. Nusrat, M.K. Siddiqi, G. Badr, M.H. Mahmoud, R.H. Khan, Insight into the interaction of antitubercular and anticancer compound clofazimine with human serum albumin: spectroscopy and molecular modelling, J. Biomol. Struct. Dyn. (2016) 1–12.
[44] M. Ishtikhar, A. Khan, C.K. Chang, L.T. Lin, S.S. Wang, R.H. Khan, Effect of guanidine hydrochloride and urea on the interaction of 6-thioguanine with human serum albumin: a spectroscopic and molecular dynamics based study, J. Biomol. Struct. Dyn. 34 (2016) 1409–1420.
[45] M.V. Khan, G. Rabbani, E. Ahmad, R.H. Khan, Fluoroalcohols-induced modulation and amyloid formation in conalbumin, Int. J. Biol. Macromol. 70 (2014) 606–614.
[46] A. Hawe, M. Sutter, W. Jiskoot, Extrinsic fluorescent dyes as tools for protein characterization, Pharm. Res. 25 (2008) 1487–1499.
[47] Y.S. Kim, T.W. Randolph, M.C. Manning, F.J. Stevens, J.F. Carpenter, Congo red populates partially unfolded states of an amyloidogenic protein to enhance aggregation and amyloid fibril formation, J. Biol. Chem. 278 (2003) 10842–10850.
[48] R. Mishra, R. Seckler, R. Bhat, Efficient refolding of aggregation-prone citrate synthase by polyol osmolytes: how well are protein folding and stability aspects coupled? J. Biol. Chem. 280 (2005) 15553–15560.
[49] Z. Ignatova, L.M. Gierasch, Inhibition of protein aggregation in vitro and in vivo by a natural osmoprotectant, Proc. Natl. Acad. Sci. U. S. A. 103 (2006) 13357–13361.
[50] S. Sukenik, D. Harries, Insights into the disparate action of osmolytes and macromolecular crowders on amyloid formation, Prion 6 (2011) 26–31.
[51] A. Natalello, J. Liu, D. Ami, S.M. Doglia, A. de Marco, The osmolyte betaine promotes protein misfolding and disruption of protein aggregates, Proteins 75 (2009) 509–517.
[52] B. van den Berg, R.J. Ellis, C.M. Dobson, Effects of macromolecular crowding on protein folding and aggregation, EMBO J. 18 (1999) 6927–6933.
[53] H.M. POHegg, B. Löfqvist, The protective effect of sodium dodecylsulphate on the thermal precipitation of conalbumin. a study on thermal aggregation and denaturation, J. Sci. Food Agric. 29 (1978) 245–260.
[54] C.R. Prabha, C. Mohan Rao, Oxidative refolding of lysozyme in trifluoroethanol (TFE) and ethylene glycol: interfering role of preexisting alpha-helical structure and intermolecular hydrophobic interactions, FEBS Lett. 557 (2004) 69–72.
[55] L. Wang, D. Schubert, M.R. Sawaya, D. Eisenberg, R. Riek, Multidimensional structure-activity relationship of a protein in its aggregated states, Angew. Chem. Int. Ed. Engl. 49 (2010) 3904–3908.
[56] M.G.S.Y. Vincent Vagenende, Bernhardt L. Trout, Mechanisms of protein stabilization and prevention of protein aggregation by glycerol, Biochemistry 48 (2009) 11084–11096.
[57] L.S. Wolfe, M.F. Calabrese, A. Nath, D.V. Blaho, A.D. Miranker, Y. Xiong, Protein-induced photophysical changes to the amyloid indicator dye thioflavin T, Proc. Natl. Acad. Sci. U. S. A. 107 (2010) 16863–16868.
[58] A. Bavdek, R. Kostanjsek, V. Antonini, J.H. Lakey, M. Dalla Serra, R.J. Gilbert, G. Anderluh, pH dependence of listeriolysin O aggregation and pore-forming ability, FEBS J. 279 (2012) 126–141.
[59] R.a.R. Srinivasan, Role of physical forces in hydrophobic interaction chromatography, Sep. Purif. Rev. 9 (1980) 267–370.
[60] D. Hall, A.P. Minton, Macromolecular crowding: qualitative and semiquantitative successes, quantitative challenges, Biochim. Biophys. Acta 1649 (2003) 127–139.
[61] L. Larini, J.E. Shea, Double resolution model for studying TMAO/water effective interactions, J. Phys. Chem. B 117 (2013) 13268–13277.
[62] B.R. Kaushik JK, Thermal stability of proteins in aqueous polyol solutions: role of the surface tension of water in the stabilizing effect of polyols, J. Phys. Chem. 102 (1998) 7058–7066.
[63] G. Xie, S.N. Timasheff, Mechanism of the stabilization of ribonuclease A by sorbitol: preferential hydration is greater for the denatured then for the native protein, Protein Sci. 6 (1997) 211–221.
[64] A. Priev, A. Almagor, S. Yedgar, B. Gavish, Glycerol decreases the volume and compressibility of protein interior, Biochemistry 35 (1996) 2061–2066.
[65] P.V. Mathew S, Polyhydric alcohols mediated inhibition of calcium activated adenosine triphosphatase activity of fish skeletal muscle actomyosin, Int. J. Food Prop. 8 (2005).